An Investigation of the Dragonfly Mission Aeroshell/Parachute Dynamics through Subscale Drop Tests

Juan R. Cruz,[1] Justin A. Shafner,[2] Brian E. Duvall,[3]
Matthew N. Gray,[4] Imran A. Khasawneh,[5] Christopher B. Meek,[6] Jody E. Miller[7]
NASA Langley Research Center, Hampton, Virginia 23681-2199

and

Brayden L. Chamberlain,[8]
ViGYAN Inc., Hampton, Virginia 23666-1325

The Dragonfly mission will place a rotorcraft/lander on Titan by 2034. The entry, descent, and landing system of the Dragonfly mission includes two parachutes: a drogue and a main. To provide needed data, subscale drop tests were used to conduct an experimental investigation of the aeroshell/parachute dynamics. The drop tests used a Disk-Gap-Band drogue parachute and two types of Ringslot main parachutes. All tests used a representative aeroshell which included the heatshield. All models were geometrically scaled to 16.7 percent. The model aeroshell had a diameter of 0.75 m. The model parachute nominal diameters were 0.9 m for the drogue and 2.78 m for the main. The aeroshell's mass properties were dynamically scaled to simulate flight at an altitude of 4 km at Titan. This dynamic scaling allowed the conversion of model test results to full-scale Titan conditions. Onboard instrumentation on the aeroshell provided data on the rotation rates, from which the Euler angles were determined. Tests were conducted by lifting the models with a drone to an altitude of 350 m and dropping them inverted. Key results from these tests were: 1) the models were able to recover from the extreme inverted initial condition and settle to low-amplitude oscillations; 2) ninety nine percent of the time the oscillation amplitudes observed with the drogue parachute were 11.4 degrees or less; 3) ninety nine percent of the time the oscillation amplitudes observed with the 20 percent porosity main parachute were 15.4 degrees or less.

[1] Aerospace Engineer, Atmospheric Flight and Entry Systems Branch, AIAA Associate Fellow, Mail Stop 489.
[2] Aerospace Engineering Research Student Trainee, Atmospheric Flight and Entry Systems Branch, Member AIAA, Mail Stop 489.
[3] Robotics and Automation Engineer, Aeronautics Systems Engineering Branch, Mail Stop 238.
[4] Electrical Engineer, Aeronautics Systems Engineering Branch, Mail Stop 238, Member AIAA.
[5] Robotics and Automation Engineer, Aeronautics Systems Engineering Branch, Mail Stop 238.
[6] Mechanical Engineer, Aeronautics Systems Engineering Branch, Mail Stop 238.
[7] Electronics Technician, Aeronautics Systems Engineering Branch, Mail Stop 238.
[8] Research Engineer, 30 Research Drive.

Nomenclature

D_{A}	=	aeroshell diameter
D_0	=	parachute nominal diameter
g	=	acceleration of gravity
h	=	altitude
I	=	mass moment of inertia
I_{xx}, I_{yy}, I_{zz}	=	aeroshell mass moments of inertia about the (x, y, z) axes, respectively
L	=	linear dimension
L_{R}	=	riser length
L_{S}	=	suspension lines length
M	=	Mach number
m	=	mass
N	=	scaling factor
N_g	=	acceleration of gravity scaling factor
N_I	=	mass moment of inertia scaling factor
N_L	=	linear dimension scaling factor
N_m	=	mass scaling factor
N_{Re}	=	Reynolds number scaling factor
N_t	=	time scaling factor
N_μ	=	dynamic viscosity scaling factor
N_ρ	=	atmospheric density scaling factor
N_ω	=	rotation rates scaling factor
p, q, r	=	aeroshell rotation rates about the (x, y, z) axes, respectively
Re	=	Reynolds number
t	=	time
V	=	velocity
x, y, z	=	aeroshell coordinate system with origin at its center of mass; z is coincident with the axis of symmetry of the aeroshell, positive pointing towards the nose
$x_{\mathrm{TB}}, y_{\mathrm{TB}}$	=	(x, y) location of the triple bridle attachment points in the aeroshell coordinate system
γ	=	flight path angle (positive above the horizon)
Θ	=	Nadir angle; angle made between the aeroshell's axis of symmetry (z) and the local vertical
μ	=	coefficient of dynamic viscosity
ξ_{CoM}	=	distance from the nose of the aeroshell to its center of mass
ξ_{TB}	=	distance from the rear surface of the aeroshell to the triple bridle confluence point
ρ	=	atmospheric density
ψ, θ, ϕ	=	standard aerospace Euler angles in the order listed about the (z, y, x) axes, respectively
Ω	=	combined pitch and roll rotation rates
ω	=	rotation rate

Subscripts

F	=	related to the full-scale vehicle
M	=	related to the model

Abbreviations

APL	=	Johns Hopkins University Applied Physics Laboratory
ASNA	=	Airborne Systems of North America
DGB	=	Disk-Gap-Band (parachute type)
E	=	entry time
EDL	=	Entry, Descent, and Landing
IMU	=	Inertial Measurement Unit
LMS	=	Lockheed Martin Space
PDS	=	Parachute Decelerator Subsystem

I. Background

NASA selected the Dragonfly mission[9] under the New Frontiers Program. This mission intends to place a rotorcraft/lander (subsequently denoted as "lander") on the surface of Titan (Saturn's largest moon) to study its prebiotic chemistry and habitability. Launch is scheduled for 2028, with arrival at Titan by 2034. The mission is led by the Johns Hopkins University Applied Physics Laboratory (APL). Other partners in this mission include Lockheed Martin Space (LMS), providing the entry aeroshell, NASA, leading the entry, descent, and landing (EDL) system development, and Airborne Systems of North America (ASNA), providing the parachute decelerator subsystem (PDS).

The current[10] Dragonfly EDL concept of operation is shown in Figure 1 (all numeric values are approximate). Prior to entry, the cruise stage separates from the aeroshell. The entry mass not-to-exceed value (including aeroshell, lander, and other systems) is estimated to be 2500 kg. The entry is ballistic. During entry, after the aeroheating and deceleration pulses are over, a drogue parachute is deployed by a mortar. This deployment occurs at a nominal Mach number of 1.5. The drogue parachute is a scaled version of the *Viking* Disk-Gap-Band (DGB) parachute with a nominal diameter of 5.4 m. To minimize interactions between the aeroshell's aerodynamic wake and the parachute, the skirt of the inflated drogue parachute is 10 aeroshell diameters (45 m) downstream of the aeroshell's maximum diameter. The first purpose of the drogue parachute is to stabilize and decelerate the aeroshell at supersonic, transonic, and subsonic speeds. After descending under the drogue parachute for approximately 104 minutes, at an altitude of approximately 4 km above the surface, the drogue parachute performs its second purpose – serving as a pilot parachute for the deployment of the main parachute. This deployment occurs at a nominal airspeed and dynamic pressure of 5.8 m/s and 78.4 Pa, respectively. The main parachute is of the 20° Conical Ringslot type and has a nominal diameter of 16.7 m. The main parachute has several purposes: 1) to provide sufficient ballistic coefficient difference for the heatshield and lander separation events, 2) to reduce the dynamic motions of the aeroshell, and 3) to deliver the lander to the desired separation vertical velocity of 2.9 m/s at an altitude above the surface of approximately 1.2 km. The time

[9] See https://www.nasa.gov/dragonfly and https://dragonfly.jhuapl.edu for more information on the Dragonfly mission.

[10] The Dragonfly mission EDL system continues to evolve. The information presented here was current at the time the tests were planned.

from main parachute deployment to lander separation is approximately 18 minutes. Powered flight starts after lander separation, followed by the first landing.

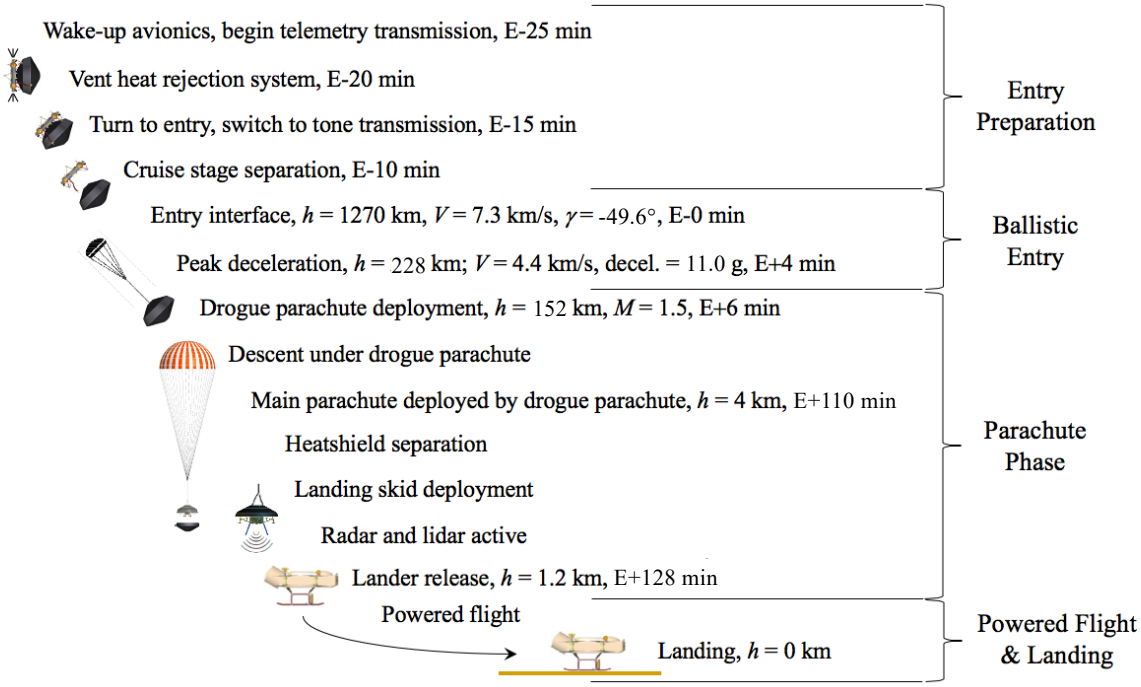

Figure 1. Dragonfly EDL Concept of Operation

One of the concerns related to the parachute phase is the dynamic behavior of the aeroshell. Excessive dynamics (i.e., large oscillation angles or rates) may be detrimental to the system at key points during the descent, including the transition from drogue to the main parachutes, heatshield release, and lander release.

II. Test Objectives

The principal objective for the drop tests described in this paper was to quantify the dynamics of the aeroshell while under the drogue and main parachute at an equivalent altitude at Titan of 4 km (i.e., at the altitude where the drogue-to-main parachute transition occurs). To achieve this objective the rotation rates, nadir angle, and Euler angles of the aeroshell were determined using data from an onboard inertial measurement unit (IMU) as described below.

III. Test Setup and Execution

A. Configurations

The test program was conducted in two phases. Phase I used the DGB drogue parachute. Phase II used two versions of the 20° Conical Ringslot main parachute with geometric porosities of 15 and 20 percent. The same aeroshell shape (including the heatshield) was used during both Phases. This aeroshell approximates the geometry of that being used by the Dragonfly mission.

B. Model Scaling

The models were geometrically-scaled to 16.67 percent. This geometric scaling was applied to the aeroshell and parachutes (including the triple bridle and single riser). The center of mass of the aeroshell was maintained at the correct geometrically-scaled location. The mass properties of the aeroshell (i.e., mass and moments of inertia) were dynamically scaled. Key scaling factors are given in Table 1. In this table N is a dimensionless scaling factor, defined as the ratio of the model value to the full-scale value. The subscript of N specifies the quantity being scaled. For example, N_L is the model to full-scale scaling factor for linear dimensions, L. For particular quantities, the subscripts M and F are used to specify model or full-scale, respectively. For example, L_{M} is a linear dimension for the model, and L_{F} is the corresponding linear dimension in full-scale.

C. Aeroshell Model

The full-scale aeroshell diameter, $(D_{\mathrm{A}})_{\mathrm{F}}$, is 4.50 m. Thus, given that $N_L = 0.1667$, the model aeroshell diameter, $(D_{\mathrm{A}})_{\mathrm{M}}$, was 0.75 m. Details of the model aeroshell geometry are shown in Figure 2. The geometry of the model aeroshell is that of the Genesis aeroshell (Ref. 1). This geometry was the starting point for the Dragonfly aeroshell geometry. Differences between the Dragonfly and Genesis aeroshell geometries are small.

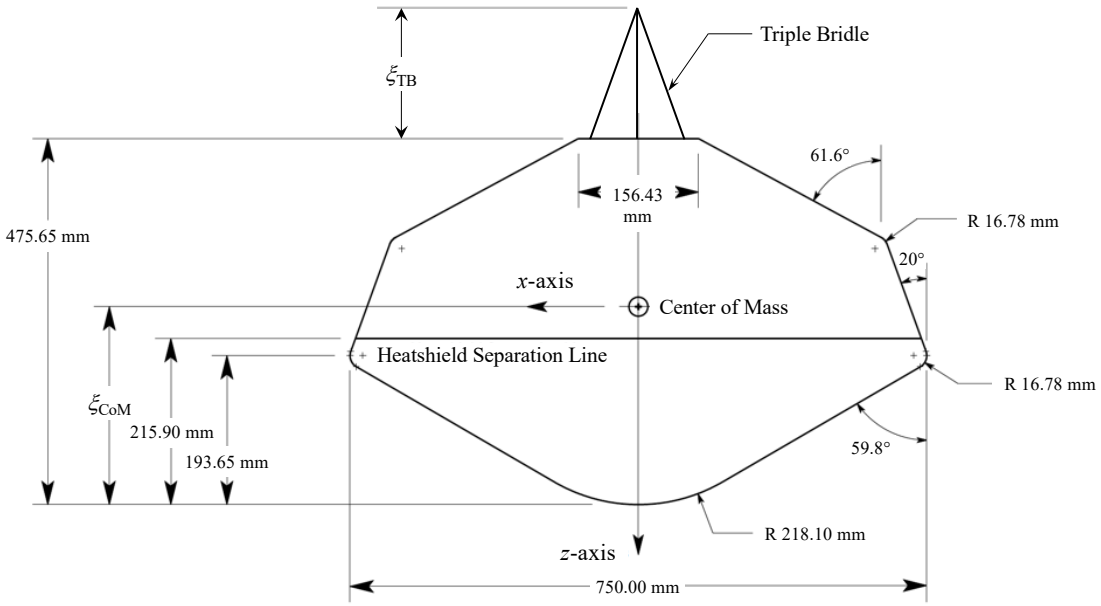

Figure 2. Model aeroshell geometry

The mass properties for the aeroshell (full-scale and models) are presented in Table 2. Scaling of the mass properties was done using the scaling factors in Table 1.

For Phase I, the aeroshell outer shells were fabricated from home insulation foam. For Phase II, the aeroshell outer shells were fabricated from epoxy-impregnated Kevlar fabric laid up in purpose-built female molds. Additional components for both sets of aeroshells were fabricated from carbon-epoxy, plastic-printed parts, and steel ballast (to meet the desired mass properties).

Table 1. Scaling factors

Parameter Type	Scale Factor	Equation	Value	Comment
Geometric	Linear Dimension	$N_L = \frac{L_\mathrm{M}}{L_\mathrm{F}}$	0.1667	16.67 percent scale model
Environment	Atmospheric Density	$N_\rho = \frac{\rho_\mathrm{M}}{\rho_\mathrm{F}}$	0.2625	$\rho_\mathrm{M} = 1.2250\ \mathrm{kg/m^3}$ (Earth sea-level) $\rho_\mathrm{F} = 4.6671\ \mathrm{kg/m^3}$ (Titan at 4 km altitude)
Environment	Acceleration of Gravity	$N_g = \frac{g_\mathrm{M}}{g_\mathrm{F}}$	7.270	$g_\mathrm{M} = 9.807\ \mathrm{m/s^2}$ (Earth sea-level) $g_\mathrm{F} = 1.349\ \mathrm{m/s^2}$ (Titan at 4 km altitude)
Environment	Dynamic Viscosity	$N_\mu = \frac{\mu_\mathrm{M}}{\mu_\mathrm{F}}$	3.059	$\mu_\mathrm{M} = 1.789 \bullet 10^{-5}$ Pa • s (Earth sea-level) $\mu_\mathrm{F} = 5.850 \bullet 10^{-6}$ Pa • s (Titan at 4 km altitude)
Mass	Mass	$N_m = \frac{m_\mathrm{M}}{m_\mathrm{F}} = N_\rho N_L^3$	$1.215 \bullet 10^{-3}$	
Mass	Mass Moment of Inertia	$N_I = \frac{I_\mathrm{M}}{I_\mathrm{F}} = N_\rho N_L^5$	$3.375 \bullet 10^{-5}$	
Time	Time	$N_t = \frac{t_\mathrm{M}}{t_\mathrm{F}} = \sqrt{\frac{N_L}{N_g}}$	0.1514	Time is compressed in model scale ($N_t < 1$).
Time	Rotation Rate	$N_\omega = \frac{\omega_\mathrm{M}}{\omega_\mathrm{F}} = \sqrt{\frac{N_g}{N_L}}$	6.604	Rotation rates of model are larger than full-scale.
Fluid Dynamics	Reynolds Number	$N_{Re} = \frac{Re_\mathrm{M}}{Re_\mathrm{F}} = \frac{N_\rho}{N_\mu}\sqrt{N_g N_L^3}$	$1.574 \bullet 10^{-2}$	Reynolds number for the model is 1.6 percent that of the full-scale.

Table 2. Full-scale and model mass properties

Property	Phase I		Phase II	
	Full-scale	Model	Full-scale	Model
Mass, m (kg)	2500	3.038	2500	3.038
Mass moment of inertia, I_{xx} (kg•m^2)	2855	0.0964	2770	0.0935
Mass moment of inertia, I_{yy} (kg•m^2)	3589	0.1212	3376	0.1140
Mass moment of inertia, I_{zz} (kg•m^2)	4366	0.1474	3814	0.1287
Center of mass location, ξ_{CoM} (m)	1.494	0.2490	1.579	0.2631

Notes to Table 2

1) The origin of the aeroshell's (x, y, z) coordinate system is at the aeroshell's center of mass as shown in Figure 2.
2) The quantity ξ_{CoM} specifies the location of the aeroshell's center of mass with respect to its nose as shown in Figure 2. The dimensionless center of mass location $\xi_{\mathrm{CoM}}/D_{\mathrm{A}}$ were 0.332 for Phase I and 0.351 for Phase II.
3) Phases I and II were conducted a year apart. During that time period the mass moments of inertia and center of mass location estimates for the aeroshell changed. These changes are reflected in Table 2.
4) The mass properties shown for the models were target values. Actual mass properties for the models were slightly different.

D. Parachute Models

Phase I was conducted using the drogue parachute. The full-scale nominal diameter of the drogue parachute, $(D_0)_{\mathrm{F}}$, was 5.40 m.[11] Thus, given that $N_L = 0.1667$, the model drogue parachute nominal diameter, $(D_0)_{\mathrm{M}}$, was 0.90 m. Both full-scale and model drogue parachutes are of the DGB type, using geometrically scaled proportions from the parachute used by the *Viking* mission. The ratio of the suspension lines length, L_{S}, to the nominal diameter, D_0, for the model drogue parachute was the same as that for the full-scale drogue parachute ($L_{\mathrm{S}}/D_0 = 1.7$). The model drogue parachutes were fabricated using 37.3 g/m^2 (1.1 oz/yd^2) parachute fabric. The model drogue parachutes had a mass of approximately 39 g.

Phase II was conducted using the main parachute. The full-scale nominal diameter of the main parachute, $(D_0)_{\mathrm{F}}$, is 16.7 m. Thus, given that $N_L = 0.1667$, the model main parachute nominal diameter, $(D_0)_{\mathrm{M}}$, was 2.78 m. Both full-scale and model main parachutes are of the 20° Conical Ringslot type. The ratio of the suspension lines length, L_{S}, to the nominal diameter, D_0, for the model main parachute was the same as that for the full-scale main parachute ($L_{\mathrm{S}}/D_0 = 1.0$). The model main parachutes were fabricated using the same low-permeability parachute fabric that is being used for the full-scale main parachutes. The model main parachutes had a mass of approximately 274 g.

[11] At the time this paper was written the drogue parachute nominal diameter is 8.25 m.

It was not possible to perfectly scale the model parachutes. Following are some of the compromises that had to be made.

1) The model parachutes had a different number of suspension lines.
2) The mass of the model parachutes was higher than their desired dynamically scaled values.
3) The fabric permeability for the drogue parachute was not correctly scaled. For the main parachute the effect of fabric permeability is minimal – both the full-scale and model main parachutes use low-permeability fabric.

These compromises were considered to be acceptable and insufficient to significantly affect the results.

E. Triple Bridle, Riser, and Trailing Distance

The parachute is attached to the aeroshell through a triple bridle and a riser. An example of this attachment is shown in Figure 3 for the drogue parachute (Phase I). The triple bridle was attached at three locations on the rear surface of the aeroshell. The locations of these attachment points $(x_{\mathrm{TB}}, y_{\mathrm{TB}})$, as well as the triple bridle confluence point, ξ_{TB}, are provided in Table 3. The riser length, L_{R}, is also given in Table 3. The triple bridle and riser lengths were scaled by the factor N_L from the dimensions of the full-scale aeroshell/parachute.

For aerodynamic reasons, the trailing distance of the parachute was fixed to a specific value. The trailing distance is defined as the distance from the aeroshell's maximum diameter to the skirt of the drogue parachute canopy when it is fully stretched-out along the axis of symmetry of the aeroshell. Trailing distance is often expressed in dimensionless terms as the ratio of the trailing distance to the aeroshell diameter. For the drogue parachute the dimensionless trailing distance was ten. For the main parachute the dimensionless trailing distance was eight.

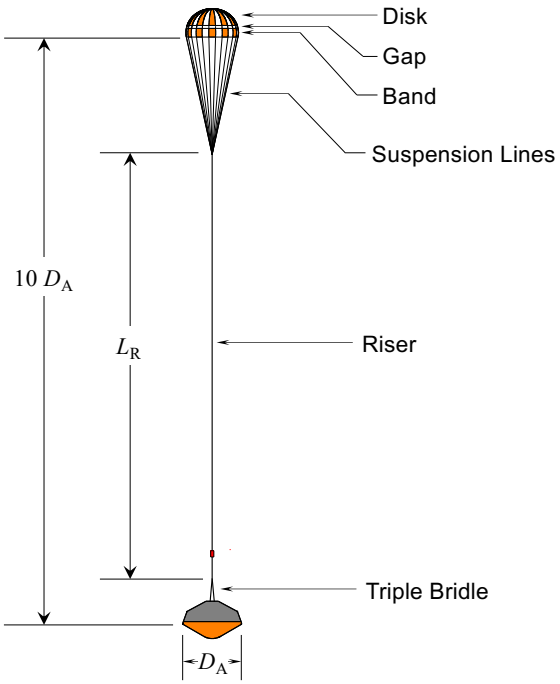

Figure 3. Attachment of the drogue parachute to the aeroshell (Phase I)

Table 3. Triple bridle and riser geometry (models)

Phase I				Phase II			
Triple Bridle Attachment Points at Aeroshell		Triple Bridle Confluence Point	Riser Length	Triple Bridle Attachment Points at Aeroshell		Triple Bridle Confluence Point	Riser Length
x_{TB} (mm)	y_{TB} (mm)	ξ_{TB} (mm)	L_R (m)	x_{TB} (mm)	y_{TB} (mm)	ξ_{TB} (mm)	L_R (m)
-76.0	0.0	290.0	5.398	66.7	0.0	252.8	2.685
-38.0	65.8			-33.3	57.7		
-38.0	-65.8			-33.3	-57.7		

Notes to Table 3

1) The origin of the aeroshell's (x, y, z) coordinate system is at the aeroshell's center of mass as shown in Figure 2.
2) The triple bridle attachment points at the aeroshell (x_{TB}, y_{TB}) are given in the aeroshell's coordinate system. These points are on the rear surface of the aeroshell as shown in Figure 2.
3) The triple bridle confluence point is located at $x = 0$, $y = 0$, at a distance ξ_{TB} aft of the rear surface of the aeroshell (see Figure 2).
4) The riser length, L_R, is the distance from the triple bridle confluence point to the parachute suspension lines confluence point (see Figure 3).

F. Instrumentation and Data Collected

The onboard instrumentation consisted of an mRobotics Control Zero F7 data recorder that includes an IMU and magnetometer. In addition, a BMP338 barometer was included. Data were stored in a microSD 32 GB card. Power was provided by two 2S 1300 mAh Lithium-Polymer batteries. The IMU was installed at the center of mass of the aeroshell. Temperature calibration of the IMU improved the accuracy of the results. The data collected are shown in Table 4. From these data other quantities were calculated.

Table 4. Data collected

Measurement	Rate
Acceleration, 3-axis	200 Hz
Rotation Rates, 3-axis	200 Hz
Magnetometer, 3-axis	200 Hz
Static Pressure	10 Hz
Euler Angles (calculated)	10 Hz

G. Test Operations

Test operations were conducted at a private airport close to the NASA Langley Research Center (this airport is near sea-level). Drops were conducted using an Alta-X drone (see Figure 4). The aeroshells were mounted inverted (i.e., heatshield up) under the drone. Dropping the aeroshell inverted allowed for verification that the aeroshell/parachute system would reach a dynamically reasonable steady-state under adverse initial conditions. The test procedure was as follows:

1) The drone was flown to an altitude of 350 m above the ground.
2) The aeroshell was released inverted.
3) As the aeroshell dropped, it pulled and deployed the riser, suspension lines, and parachute (in that order).
4) The parachute inflated.
5) The aeroshell descended under parachute. For the drogue parachute, descent time was approximately 45 s. For the main parachute, descent time was approximately 80 s.
6) The model landed and was retrieved. The on-board data was downloaded.
7) The model was reset for another drop.

Figure 4. Test operations (Phase II)

IV. Data Analyses and Results

A. Available Data

Phase I testing was conducted during November and December of 2022 over three days. Twelve drop tests were conducted using three aeroshell models and four drogue parachute models. A total of 6.8 minutes of quasi-steady state descent data were acquired, representing the equivalent[12] of 45 minutes on Titan.

Phase II testing was conducted during October and November of 2023 over four days. A total of 25 drops were conducted, 12 with the main parachutes of 15 percent geometric porosity, and 13 with the main parachutes of 20 percent geometric porosity. Three aeroshell models and six main parachutes (three each of 15 percent and 20 percent geometric porosity) were used. A total of 16.6 minutes of quasi-steady state descent data were acquired for the 15 percent geometric porosity model parachutes, representing the equivalent of 110 minutes on Titan. A total of 16.5 minutes of quasi-steady state descent data were acquired for the 20 percent geometric porosity model parachutes, representing the equivalent of 109 minutes on Titan.

B. Data Segmentation

The on-board instrumentation recorded data from several minutes before drone takeoff to several minutes after the aeroshell's landing. A partial record of the rotation rates and Euler angles recorded for a Phase I drop is shown in Figure 5. In this figure the drop starts at $t = 1331$ s.

[12] See Table 1 for the time scale factor.

Because the aeroshell is released inverted and the parachute has to deploy and inflate, a significant high-dynamic period is observed for approximately 15 s. By $t = 1346$ s the dynamics have stabilized to a quasi-steady state. The period of interest to quantify the dynamics is labeled "Quasi-steady state descent" in Figure 5. On some drops a temporary increase in the dynamics were observed during quasi-steady state descent. These events are probably related to atmospheric turbulence. One such temporary event is noted in Figure 5.

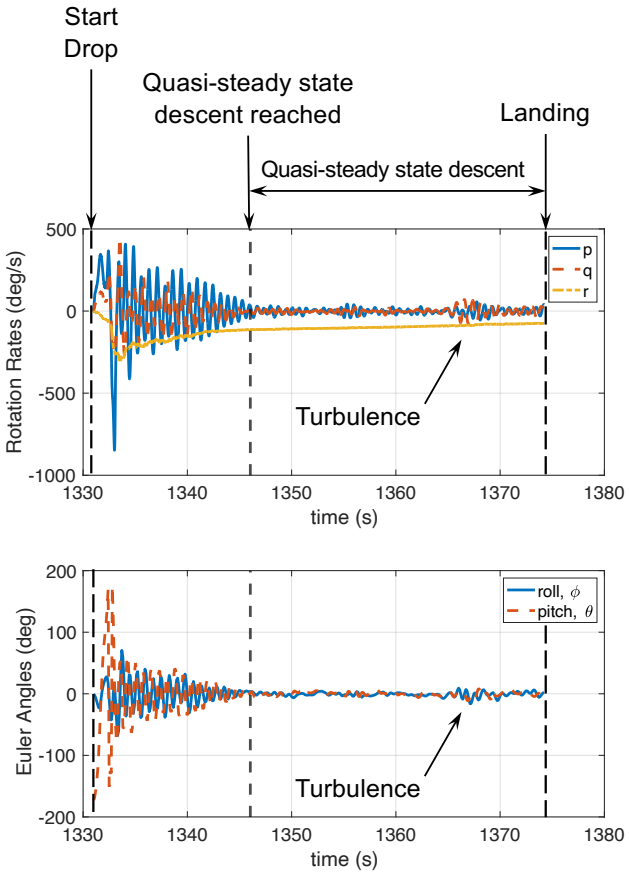

Figure 5. Sample data.

C. Results

The following results of interest were selected to describe the dynamics of the aeroshell.

1) The absolute values of the Euler angles θ and ϕ about the y- and x-axes, respectively. (This paper uses standard aerospace Euler angles (ψ, θ, ϕ) in the order listed, about the (z, y, x) axes, respectively. The azimuth Euler angle ψ was not of interest to the present work. Beware that in other literature the aeroshell axis of symmetry is the x-axis.)
2) The Nadir angle Θ. This is the angle made between the aeroshell's axis of symmetry (z) and the local vertical (see Figure 6) and calculated using the equation $\Theta = \cos^{-1}[\cos(\theta)\cos(\phi)]$ where $0° \leq \Theta \leq 180°$.
3) The rotation rates q and p about the about the y- and x-axes, respectively.
4) The combined rotation rate $\Omega = \sqrt{q^2 + p^2}$.

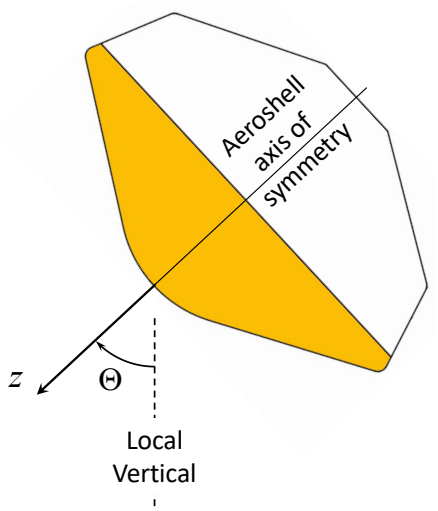

Figure 6. Definition of the nadir angle Θ

The time histories of $|\theta|$, $|\phi|$, Θ, $|q|$, $|p|$, and Ω for all tests of a given parachute type were combined and used to calculate percentiles of their distributions. These percentiles are presented in Tables 5 and 6. For rotation rate quantities (i.e., q, p, and Ω), their values, as obtained from the on-board model instrumentation, was scaled by N_ω to yield the related full-scale values. Note that the percentiles for θ, ϕ, q, and p were calculated on their absolute values because, for the purpose of this investigation, positive and negative values have the same dynamic consequences. Because Θ and Ω are always positive, there was no need to calculate their absolute values. When calculating the percentiles for Θ and Ω, their time histories were calculated first by combining their component quantities (i.e., θ and ϕ for Θ, and q and p for Ω), and then calculating the percentiles. The 99%-tile values were the most relevant to the Dragonfly mission and are discussed below; the other percentiles and maximum values are presented to provide a sense of the cumulative probability distributions.

From the results shown in Tables 5 and 6, the following observations, focusing on the 99%-tile values, can be made.

1) The differences between the pitch and roll rates and angles (i.e., $|\theta|$ and $|\phi|$, and $|q|$ and $|p|$) were small for both the drogue and main parachutes. This was expected due to the high level of axial symmetry of the aeroshell/parachute models.
2) The drogue parachute had lower values of $|\theta|$, $|\phi|$, and Θ than the main parachutes.
3) The 20 percent geometric porosity main parachute had lower values of $|\theta|$ and $|\phi|$, and Ω than the 15 percent geometric porosity main parachute. This was expected; all other things being equal, increasing the geometric porosity of a parachute often improves its dynamic characteristics.
4) The drogue parachute had higher values of $|q|$, $|p|$, and Ω than the main parachutes.
5) The 20 percent geometric porosity main parachute had lower values of $|q|$, $|p|$, and Ω than the 15 percent geometric porosity main parachute. Again, this was expected.
6) For all parachutes, the values of $|q|$, $|p|$, and Ω were low.

Table 5. Statistics for $|\theta|$, $|\phi|$, and Θ

Percentile	Phase I			Phase II					
	Drogue Parachute			Main Parachute 15% Geometric Porosity			Main Parachute 20% Geometric Porosity		
	Pitch Angle $\|\theta\|$ (deg)	Roll Angle $\|\phi\|$ (deg)	Nadir Angle Θ (deg)	Pitch Angle $\|\theta\|$ (deg)	Roll Angle $\|\phi\|$ (deg)	Nadir Angle Θ (deg)	Pitch Angle $\|\theta\|$ (deg)	Roll Angle $\|\phi\|$ (deg)	Nadir Angle Θ (deg)
50%-tile	2.0	2.0	3.6	5.0	4.8	8.6	2.9	3.3	5.5
90%-tile	5.2	5.4	7.0	11.4	11.2	14.3	8.0	7.7	10.6
99%-tile	**9.4**	**9.3**	**11.4**	**16.7**	**15.7**	**18.2**	**13.1**	**12.7**	**15.4**
Maximum	14.3	24.2	24.5	21.5	21.4	23.9	21.9	19.5	22.7

Table 6. Statistics for $|q|$, $|r|$, and Ω (full-scale)

Percentile	Phase I			Phase II					
	Drogue Parachute			Main Parachute 15% Geometric Porosity			Main Parachute 20% Geometric Porosity		
	Pitch Rate $\|q\|$ (deg/s)	Roll Rate $\|p\|$ (deg/s)	Combined Pitch and Roll Rates Ω (deg/s)	Pitch Rate $\|q\|$ (deg/s)	Roll Rate $\|p\|$ (deg/s)	Combined Pitch and Roll Rates Ω (deg/s)	Pitch Rate $\|q\|$ (deg/s)	Roll Rate $\|p\|$ (deg/s)	Combined Pitch and Roll Rates Ω (deg/s)
50%-tile	1.6	1.7	2.8	1.1	1.1	2.0	0.8	0.7	1.3
90%-tile	4.1	4.1	5.4	2.6	2.6	3.3	1.9	1.9	2.6
99%-tile	**7.7**	**6.9**	**9.2**	**4.0**	**3.9**	**4.5**	**3.4**	**3.4**	**4.2**
Maximum	19.9	10.6	20.0	6.0	6.1	6.6	6.3	6.6	7.7

V. Conclusions

The tests and results described here fulfilled the needs of the Dragonfly mission. Results are being used to specify requirements for the lander and to validate flight mechanics simulations. The hardware and test procedure has matured to the point that significant amounts of useful data can be obtained with a few days of testing. This drop test technique has been shown to be useful and cost-effective. Additional drop tests are planned support the ongoing development of the Dragonfly mission.

Acknowledgments

The contributions of the following individuals from the NASA Langley Research Center are gratefully acknowledged. Richard E. Martin and Donald S. Smith, Manufacturing Applications Branch. Matthew W. Coldsnow, Jennifer W. Fowler, Mark W. Frye, Skyler J. Hudson, and Amanda D. Neff, UAS Operations Office. N. Giovanny Guecha-Ahumada, Atmospheric Flight and Entry Systems Branch. Brian D. Ferguson, Engineering Integration Branch. The models of the main parachutes were designed and fabricated by staff at ASNA.

References

1) Desai, P. N. and Cheatwood, F. M., "Entry Dispersion Analysis for the Genesis Sample Return Capsule," *Journal of Spacecraft and Rockets*, Vol. 38, No. 3, pp. 345-350, 2001.